Applied Catalysis B: Environmental 163 (2015) 591–598

Contents lists available at ScienceDirect

Applied Catalysis B: Environmental

journal homepage: www.elsevier.com/locate/apcatb

Identification of TiO_2 photocatalytic destruction byproducts and reaction pathway of cylindrospermopsin

Geshan Zhang[a], Elizabeth M. Wurtzler[a], Xuexiang He[a], Mallikarjuna N. Nadagouda[b], Kevin O'Shea[c], Said M. El-Sheikh[d], Adel A. Ismail[d], David Wendell[a], Dionysios D. Dionysiou[a,*]

[a] Environmental Engineering and Science Program, University of Cincinnati, Cincinnati, OH 45221, USA
[b] S.E.T's College of Pharmacy, Department of Pharmaceutical Engineering and Chemistry, Sangolli Rayanna Nagar, Dharwad 580 002, India
[c] Department of Chemistry and Biochemistry, Florida International University, Miami, FL 33199, USA
[d] Central Metallurgical R&D Institute, Cairo 11421, Egypt

ARTICLE INFO

Article history:
Received 2 May 2014
Received in revised form 15 August 2014
Accepted 20 August 2014
Available online 27 August 2014

Keywords:
Byproduct
Cylindrospermopsin
Detoxification
TiO_2 photocatalytic degradation
Reaction pathway

ABSTRACT

Cylindrospermopsin (CYN) has become a significant environmental concern because of its extremely high toxicity and widespread distribution. TiO_2 assisted photocatalytic degradation process has been proven to be effective for CYN degradation. However, the lack of investigation on byproducts and pathways of CYN photocatalytic destruction limited the assessment of this treatment technology (e.g. toxicity of effluent). Therefore, the reaction byproducts and pathways of CYN degradation by TiO_2 photocatalysis were studied in this work by using high-performance liquid chromatography combined with quadrupole time-of-flight electrospray ionization tandem mass spectrometry (LC/Q-TOF–ESI–MS). The reaction pathways were proposed and discussed based on the detected byproducts and hydroxyl radical chemistry. The byproducts m/z 432.12 and 448.11 can be formed through hydroxylation by $^{\bullet}OH$ hydrogen abstraction and addition to double bonds. Byproducts without the sulfate group can be generated through a sulfate elimination process. Byproducts (such as m/z 392.12 and 375.10) formed after ring opening by attacks on the hydroxymethyl uracil moiety and tricyclic guanidine moiety were also identified in this study. The detoxification study showed an effective removal of cytotoxicity after TiO_2 photocatalytic treatment. This work is important in the proper assessment of the photocatalytic destruction of CYN in water and provides insights that can help determine the level of treatment required by such advanced oxidation technologies.

1. Introduction

Cylindrospermopsin (CYN) was firstly identified as a fatal cyanotoxin after the hepatitis-like disease outbreak occurred in 1979 on Palm Island, Queensland in Australia. It is a water-soluble tricyclic guanidine alkaloid that can penetrate a wide range of cells and poison various organs of the respiratory and circulatory systems, as well as bone marrow [1–3]. It has been reported that CYN induces apoptosis by oxidative stress and protein synthesis inhibition even at nanomolar levels [4]. Furthermore, this toxin can inhibit glutathione production, which is critical to conjugation and reduction reactions within the cell, resulting in irreparable damage to the mitochondria and genome [5]. CYN is naturally produced by a variety of cyanobacterial genera (e.g. *Cylindrospermopsis*, *Umezakia*, and *Anabaena*). CYN-producing cyanobacteria have been identified in most tropical and temperate waters, including certain sources of drinking water, the latter of which is of particular concern to potable water treatment. Despite the lack of EPA regulation on CYN, due in part to its relatively recent discovery, researchers have proposed a safe guideline value of 1 μg/L in drinking water [6].

Chlorination has been proven to achieve effective oxidation and detoxification of CYN [7]. However, this process produces chlorinated disinfectant byproducts (DBPs). One alternative is the use of advanced oxidation technologies (AOTs). TiO_2 photocatalysis is one of most popular AOTs. Research has demonstrated CYN can be degraded using TiO_2 photocatalysts under UV irradiation [8]. However, to our knowledge only another very recent study has dealt with detailed reaction byproducts and pathways of TiO_2 photocatalytic degradation of CYN [9].

* Corresponding author. Tel.: +1 513 556 0724; fax: +1 513 556 4162.
E-mail addresses: dionysios.d.dionysiou@uc.edu, dionysdd@ucmail.uc.edu (D.D. Dionysiou).

http://dx.doi.org/10.1016/j.apcatb.2014.08.034
0926-3373/

The uracil moiety in the CYN toxin (Fig. S1a in Supporting information (SI)) is considered to be responsible for its deleterious effects [10]. Therefore, it is extremely important to investigate the destruction of the uracil functionality in CYN and measure the subsequent biological activity of the TiO_2 photocatalysis byproducts. In chlorination, the toxin was discovered to form 5-chloro-cylindrospermopsin and cylindrospermic acid, in which the uracil moiety was transformed and additional work has shown these two byproducts are nontoxic to mice [10]. Besides, an analog of CYN, deoxycylindrospermopsin, has been discovered to lack responsibility for the toxicity of *Cylindrospermopsis raciborskii*, indicating the presence of a hydroxyl group on C7 of CYN is also important for its toxicity [11]. Previous work has proposed reaction byproducts and pathways for the reaction of CYN and hydroxyl radicals generated from gamma radiolysis using LC–MS analysis [12]. Our previous study on UV/H_2O_2 process for CYN treatment also proposed its degradation mechanism [13]. However, limited information is available on the byproducts of CYN photocatalytic degradation [9]. Since the toxicity of the photocatalytically treated water is still unknown, it is extremely important to obtain this information for the practical application of TiO_2 photocatalysis for CYN treatment in real world applications. In order to better understand and evaluate TiO_2 photocatalysis for CYN destruction, it is necessary to identify the reaction byproducts and unveil the degradation pathways.

In this work, we report the transformation mechanisms and detailed reaction pathways of the photocatalytic destruction of CYN using TiO_2 photocatalysts (P25 and lab synthesized polymorphic TiO_2). The generated byproducts were identified by high-performance liquid chromatography combined with quadrupole time-of-flight electrospray ionization tandem mass spectrometry (LC/Q-TOF–ESI–MS). The reaction pathways and the relative cytotoxicity of the corresponding byproducts were also investigated. This study can further support the assessment of TiO_2 photocatalytic treatment of CYN from fundamental mechanism aspects.

2. Materials and methods

2.1. Materials

CYN (>95%) was purchased from GreenWater Laboratories. Aeroxide TiO_2 P25 was obtained from Evonik Degussa. Nano-size polymorphic TiO_2 (PM-TiO_2) was lab synthesized containing anatase, brookite and rutile phase TiO_2 [14]. The water applied in photocatalytic experiments was supplied by Tedia (HPLC grade). For analysis of samples from photocatalytic experiments, HPLC grade acetonitrile, deionized ultra-filtered water and glacial acetic acid (99.9%) were purchased from Fisher Scientific. In the toxicity study, all reagents were used without further purification.

2.2. TiO_2 photocatalytic experiments

In order to have detailed byproduct studies, a high initial concentration of 10 μM CYN was applied in the photocatalytic experiments. P25 or PM-TiO_2 particles were dispersed in water using ultrasonication (2510R-DH, Bransonic) to form uniform nanoparticle suspensions. CYN stock solution and catalyst suspension were added to a borosilicate glass Petri dish (Pyrex, 60 mm (*ø*) × 15 mm (*h*)) to a final volume of 10 mL and enclosed with a quartz cover. The catalyst load applied in the experiments was 0.25 g/L. The reaction suspension was also prepared with HPLC grade water without any adjustment (the pH of the reaction suspension was close to the neutral pH). The reactor was irradiated under two 15 W fluorescent lamps [14,15] (Cole-Parmer) with a light intensity of around 2.3 mW/cm^2 determined with a radiant power meter (Newport Co.). The reaction was operated under continuous stirring and temperature control. Samples (150 μL) were taken after certain reaction time intervals, diluted with 150 μL water and filtered using a syringeless filter (0.2 μm, PTFE, Whatman).

2.3. Sample analysis on LC/Q-TOF–ESI–MS

The separation of reaction byproducts from TiO_2 photocatalytic experiments was performed on an Agilent 1290 infinity HPLC system (Agilent Technologies) equipped with a Zorbax Eclipse XDB-C18 Rapid Resolution column (2.1 × 50 mm, 3.5 μm, Agilent Technologies). The mobile phase A was H_2O + 2% acetonitrile + 0.2% acetic acid and the mobile phase B was acetonitrile + 2% H_2O + 0.2% acetic acid. Gradient elution was programmed as follows: 2% B for 1 min; linearly increasing to 95% B in 4 min; dropping to 2% B in 0.1 min; and holding 2% B for 2 min for re-equilibrium. The flow rate and sample injection volume were set as 0.2 mL/min and 10 μL, respectively. The column temperature was maintained at 35 °C.

An Agilent 6540 UHD accurate-mass quadrupole time-of-flight tandem mass spectrometer (Q-TOF–MS) was coupled to the HPLC with an electrospray ionization source (ESI). The analysis was in positive ion mode for mass spectra (*m/z* 100 to 500). The parameters set for ESI–MS were: drying gas temperature 300 °C, drying gas flow 7 L/min and Nebulizer 45 psig. For MS spectrum analysis, the collision energy was ramped with a slope of 3 and an offset of 10. The TOF scan data were analyzed using Agilent MassHunter workstation software (Qualitative Analysis B.04.00) which provided a list of possible chemical formulae for targeting compounds based on mass to charge ratio (*m/z*) and isotope distribution (for best matching formulae, relative mass differences ≤5 ppm). The MS spectra were obtained under MS/MS mode. The structures of the byproducts were proposed according to their MS spectra, possible formulae and retention time (RT).

2.4. Detoxification study

Human hepatocellular carcinoma cell line C3A cells (ATCC No. CRL-10741) were maintained at 37 °C in an atmosphere containing 6% CO_2 (CO_2 incubator, Thermo Forma), in a medium consisting of Eagle's Minimum Essential Medium (EMEM, ATCC No. 30-2003) with 10% fetal bovine serum (ATCC No. 30-2020). C3A cells were diluted to 2.5 × 10^5 cells/mL and 200 μL were placed in each well of the 96-well tissue-culture plates (Corning) 24 h before exposure to CYN. The samples from the photocatalytic experiment by using P25 TiO_2 were concentrated by evaporation and then dissolved in fresh culture medium with the same volume as the samples. The culture without CYN was used as the control. The culture medium of the cells was then replaced by the medium with toxin and incubated at 37 °C for 48 h. All absorbance measurements were quantified using a FlexStation 3 Plate Reader (Molecular Devices, CA).

Total protein content (PC) was quantified as previously described [16]. Briefly, protein dissolution was achieved by replacing the culture medium with 200 μL NaOH (1 M, Fisher). After incubation at 37 °C for 2 h, 180 μL of the supernatant was replaced by Coomassie Brilliant Blue G (Sigma) solution (0.01% Coomassie Brilliant Blue G, 4.7% ethanol (≥99.5%, Sigma) and 8.5% phosphoric acid (85%, Fisher)) and after 30 min incubation at room temperature, the absorbance was quantified at 620 nm.

The Neutral Red (NR) cellular uptake test was used to check cell viability. Culture medium was removed and replaced by 100 μL serum free medium with 50 μg/mL of NR (Sigma). After 3 h incubation at 37 °C, the cells were fixed with 1% formaldehyde (37%, Fisher)–1% $CaCl_2$ (Fisher) solution for 1 min. After adding 200 μL of

acetic acid (99.9%, Fisher):ethanol:water (1:49:50) solution, the NR absorbed by the cells was extracted and measured at 540 nm [17].

In the MTS (3-(4,5-dimethylthiazol-2-yl)-5-(3-carboxymethoxyphenyl)-2-(4-sulfophenyl)-2H-tetrazolium) reduction test, CellTiter 96 AQueous One Solution Cell Proliferation Assay (Promega) was applied. Twenty microliters of the solution reagent was added into each well with 100 μL of fresh medium. After 3 h of incubation at 37 °C, the amount of colored formazan product was directly tested by measuring absorbance at 490 nm.

All experiments of the toxicity study were performed at least three times. The data from each assay were shown as the mean percentage of the results from the control experiment. Analysis of variance (ANOVA) was applied for the statistical analysis. Differences from controls were considered significant when $p \leq 0.05$.

3. Results and discussion

3.1. Photocatalytic reaction byproducts of CYN with P25 and PM-TiO_2

Using the above mentioned analysis method, CYN eluted at the retention time of 1.00 min, giving the mass spectrum as shown in Fig. S1b in SI. CYN $(M+H)^+$ ion (m/z = 416.12) can lose a SO_3 (−80 Da) from sulfate group to yield m/z 336.17 and then lose an H_2O (−18 Da) from hydroxyl group to yield an m/z 318.16 fragment ion. It can further lose the hydroxymethyl uracil moiety (−142 Da) to give an m/z 194.13 fragment ion following the loss of another H_2O to yield m/z 176.12. The m/z 274.08 fragment corresponds to the loss of hydroxymethyl uracil moiety first from the CYN $(M+H)^+$ ion. This observation is in good agreement with previous research on mass spectroscopy analysis of CYN [18].

Results from the photocatalytic degradation of CYN by using P25 and PM-TiO_2 photocatalysts are shown in Fig. S2 in SI, indicating the photocatalytic process can remove CYN efficiently. PM-TiO_2 photocatalyst is lab-made polymorphic TiO_2 with anatase (66%), brookite (22%) and rutile (12%) phases. Its physiochemical properties and photocatalytic reactivity for CYN removal in different water matrices have been reported in our previous work [14]. The pseudo-first-order rate constants for P25 and PM-TiO_2 were 0.16 and 0.03 min^{-1}, respectively, under current reaction conditions and catalyst loading. P25 performed with higher activity than the synthesized PM-TiO_2 under the conditions applied in this study, which is attributed to the different physiochemical properties of the two materials, such as the catalytic activities in the UV spectrum, role of the brookite and rutile phases in the two types of nanomaterials, and efficiency of light utilization as a function of extent of aggregation [8,14,19]. The formulae of the main reaction byproducts with each catalyst were identified and listed in Table S1 (SI). These byproducts were reported according to their peak areas from the extracted ion chromatogram (EIC), proposed formulae, mass spectra and RTs [20,21]. Most byproducts existed in both systems of P25 and PM-TiO_2. The major byproducts, which appeared continuously during the reaction time with relatively high peak areas, are displayed in Fig. S3 of SI. In both systems, the byproducts with higher molecular weights, such as m/z 448.11, 432.12 and 414.11, reached their greatest abundance at the early stage of the reaction (6 min with P25 and 40 min with PM-TiO_2). Their mass spectra and proposed structures are illustrated in Figs. S4–S6 in SI. Generally, in the mass spectra a difference of 80 Da between two fragment ions indicates the presence of a sulfate group while a difference of 18 Da suggests a hydroxyl group. The loss of the complete hydroxymethyl uracil moiety would give a difference of 142 Da. The existence of fragment m/z 194.13 suggests the integrity of the tricyclic guanidine moiety (e.g. the mass spectrum of CYN m/z = 416.12) while the fragment m/z 192.11 implies a hydroxyl group (losing one H_2O during the fragmentation) connecting to the tricyclic guanidine moiety (e.g. m/z 432.12a) or the existence of a double bond on the tricyclic guanidine moiety (e.g. byproduct m/z 414.11) [22]. The retention times of byproducts are also related to their structures. Since the retention time of the CYN parent compound was 1.00 min under the above mentioned analytical method, byproducts with higher polarity would elute earlier; byproducts with lower polarity would elute later. From the observation, the elution times of these reported byproducts are in the range of 0.7–1.8 min.

3.2. Photocatalytic reaction mechanisms of CYN with P25 and PM-TiO_2

Hydroxyl radicals (•OH) produced by TiO_2 catalysts are predominantly responsible for the degradation of organic pollutants during the photocatalytic reaction [20,23–25]. Positive holes in the valence band can be formed after electrons being excited from the valence band to conduction band when TiO_2 adsorbs a photon that has energy higher than or equal to the bandgap energy, which would further react to generate reactive hydroxyl radicals [25–28]. Hydroxyl radical can react with organic pollutants with very high second-order rate constants, most of which are from around 10^9 to 10^{10} M^{-1} s^{-1} [27,29,30]. The photocatalytic mechanism of CYN destruction by P25 and PM-TiO_2 photocatalysts discussed in this work is on the basis of hydroxyl radical attack. The main reaction mechanism of hydroxyl radicals includes hydrogen abstraction and addition to double bonds [12,31–33]. A hydroxyl radical can attack C—H bond through hydrogen abstraction to form a carbon-centered radical, which later can react with O_2 and/or •OH to yield the corresponding alcohol [20,32–34]. Eventually the oxidation can further produce the corresponding aldehyde, ketone or acid (Scheme S1, SI). The addition of hydroxyl group to C=C double bond can occur at either sp2-hybridized carbon resulting in hydroxylation and the formation of a carbon-centered radial. If resulting carbon centered radical has hydrogen attached, the addition of O_2 and subsequent release of HO_2• yields the corresponding enol or ketone [20,33]. Generally, •OH is considered as an electrophilic agent that preferentially reacts at sites with higher electron densities [35,36].

3.2.1. Hydroxylation of CYN

CYN can be hydroxylated by hydroxyl radicals through hydrogen abstraction and addition to the C=C double bond. The m/z 432.12a (CYN $(M+H)^+$ + 16 Da, Fig. S5 (a) in SI, Scheme 1) can be any hydroxylated compounds generated from the hydrogen abstraction on the carbon alpha to the nitrogen of the tricyclic guanidine moiety or to oxygen of the sulfate group (C8, C10, C12, C14 and C15) [12]. The nitrogen in the amino group and oxygen (connected to C12) in the sulfate group here played the roles of electron-donors that could promote the formation of m/z 432.12a byproduct(s) by increasing the electron density of the α-carbon groups [37–39]. Because the different positions of the hydroxyl group on the tricyclic guanidine moiety would barely affect the mass spectra, these compounds cannot be distinguished under this study. The m/z 432.12b byproduct was generated from •OH addition to the C5–C6 double bond in the uracil moiety. Fujita and Steenken found that hydroxyl radicals can add to the C5=C6 double bond of uracil and the substitution by methyl group at C6 would decrease the probability of •OH adduct at C6 and subsequently favor an addition at C5 [40]. The byproducts m/z 432.12a and 432.12b share the same m/z value but different structures based on the different mass spectra (Fig. S5, SI). This observation is consistent with previous researches [12,13]. Compounds with the same m/z value shared the same EIC spectra (Fig. S7, SI) and hence the reported formation of byproduct m/z 432.12 in Fig. S3 (SI) included both m/z 432.12a and 432.12b. The m/z 432.12a and 432.12b byproducts could undergo further

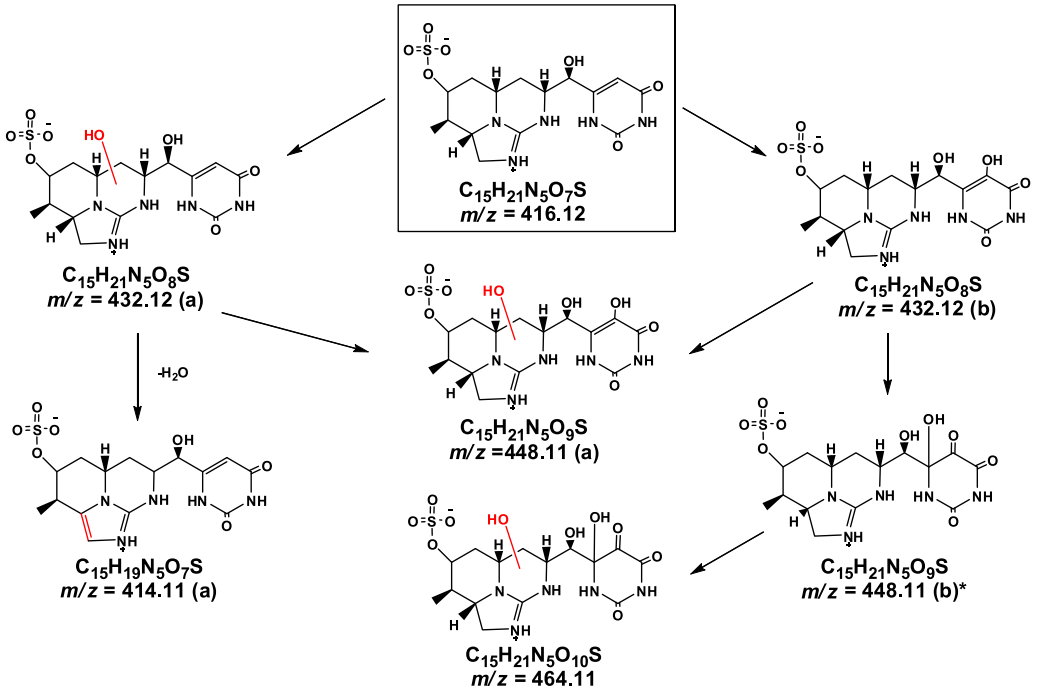

Scheme 1. Hydroxylation of CYN. (The red color indicates the group does not have a fixed position. The byproduct structure with "*" means the mass spectrum of this reaction byproduct was not detected but was possibly existing in system). (For interpretation of the references to color in this figure legend, the reader is referred to the web version of this article.)

hydroxylation to form *m/z* 448.11a (CYN $(M+H)^+$ + 32 Da, Scheme 1, Fig. S4 in SI). This structure is different from the structure proposed by Song et al. (*m/z* 448.11b) [12]. The byproduct *m/z* 448.11b may have also existed in this reaction, however, only the mass spectrum for *m/z* 448.11a was detected. The further hydroxylated byproduct *m/z* 464.11 (CYN $(M+H)^+$ + 48 Da) and 480.10 (CYN $(M+H)^+$ + 64 Da) were also detected by TOF Scan analysis. Since the uracil moiety has been reported to be essential for CYN toxicity, degradation byproducts (such as *m/z* 432.12b) with modified uracil groups may have reduced toxicity.

The byproduct *m/z* 414.11a (CYN $(M+H)^+ - 2$ Da, Fig. S6 in SI, Scheme 1) with C=C double bond can be generated through

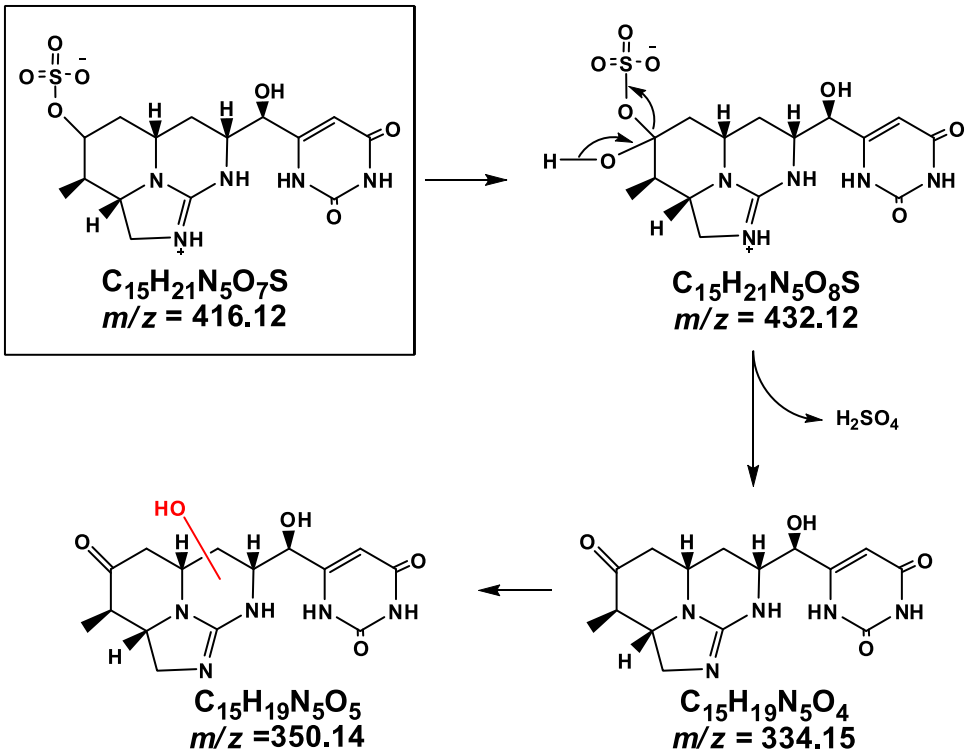

Scheme 2. Elimination of sulfate group. (The red color indicates the group does not have a fixed position). (For interpretation of the references to color in this figure legend, the reader is referred to the web version of this article.)

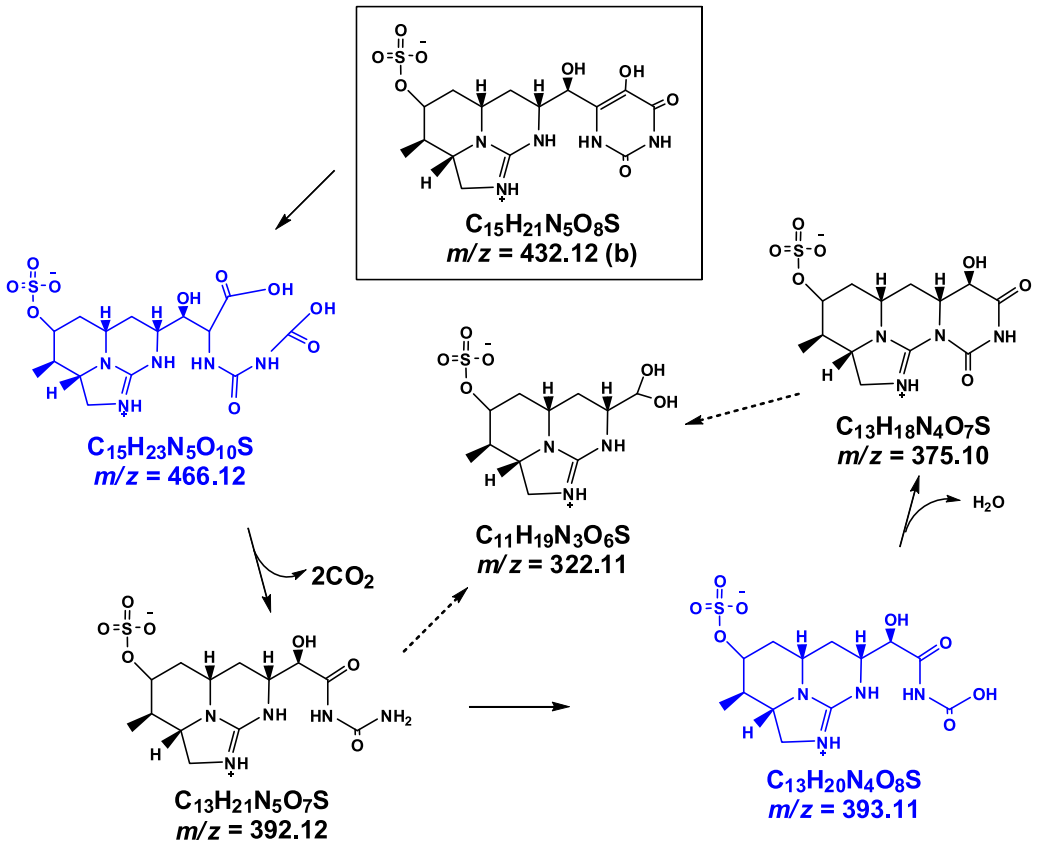

Scheme 3. Reaction on the hydroxymethyl uracil moiety. (The byproducts with blue color indicate these byproducts were not detected and were proposed based on current information.) (For interpretation of the references to color in this figure legend, the reader is referred to the web version of this article.)

dehydration from *m/z* 432.12a. C=C double bonds are usually unstable and easy to react with •OH as described before. However, this byproduct can be relatively stable in this system due to the conjugation of the guanidine group and the C=C double bond. Bachman reported a dehydrated photodecomposition byproduct of carbofuran [41], which has the conjugation structure of double bond and aromatic ring. The *m/z* 414.11a can be any compounds which were derived from the dehydration of *m/z* 432.12a byproduct(s). This byproduct is different from the one suggested in previous research (a carbonyl generated from the oxidation of secondary alcohol on the methyl bridge (C5), *m/z* 414.11b) [12]. In this study, only one mass spectrum for *m/z* 414.11a was detected. However, the existence of *m/z* 414.11b cannot be excluded because the electron-donating property of the hydroxyl group can facilitate the reaction with •OH. Moreover, this byproduct could be generated through a similar pathway as *m/z* 414.11a when the formed double bond is on C7=C8. Then the generated enol would transform to the ketone *m/z* 414.11b. Similarly, the byproduct *m/z* 446.10 was also detected by TOF Scan analysis.

3.2.2. Elimination of sulfate group

The cleavage of the sulfate group was also observed in systems with both catalysts. In the mass spectrum for *m/z* 334.15 (CYN $(M+H)^+ - 82$ Da), the loss of 80 Da was not observed, which confirmed the release of a sulfate group. The mass spectrum shows an *m/z* 192.11 fragment (loss of 142 Da) indicating the completed structure of the hydroxymethyl uracil moiety and the existence of a double bond or hydroxyl group on the tricyclic guanidine group. The absence of *m/z* 174.10 fragment in the spectrum suggests the absence of an OH group at C12. Hence the presence of C=O double bond at C12 is proposed (Scheme 2). The byproduct *m/z* 334.15 can be generated through hydroxylation and elimination of sulfuric acid (Scheme 2). Similarly, research about the phosphate cleavage of phosphate esters through the reaction with •OH [42] suggests the cleavage could occur after the hydroxylation of the carbon alpha to the phosphate group to form a ketone and release one molecule of H_3PO_4. The hydroxylation of *m/z* 334.15 can yield byproduct *m/z* 350.15, which was found to have more than one isomer (Table S1, SI). The further hydroxylation byproducts *m/z* 366.14, 382.14 and 398.13 were also detected by TOF Scan analysis. In our previous research on UV/H_2O_2 process for CYN degradation, the sulfate cleavage was also observed [13].

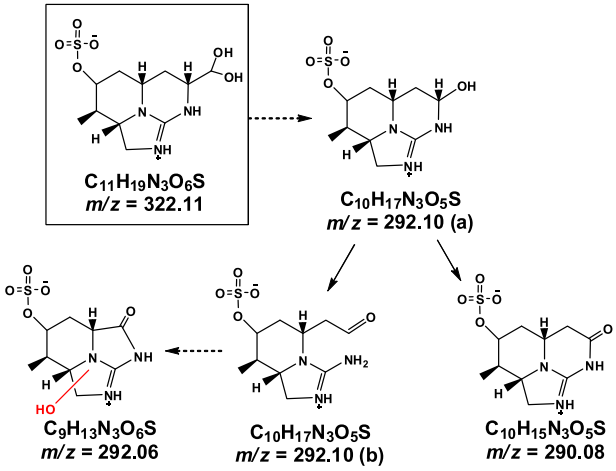

Scheme 4. Reaction on the tricyclic guanidine moiety. (The red color indicates the group does not have a fixed position.) (For interpretation of the references to color in this figure legend, the reader is referred to the web version of this article.)

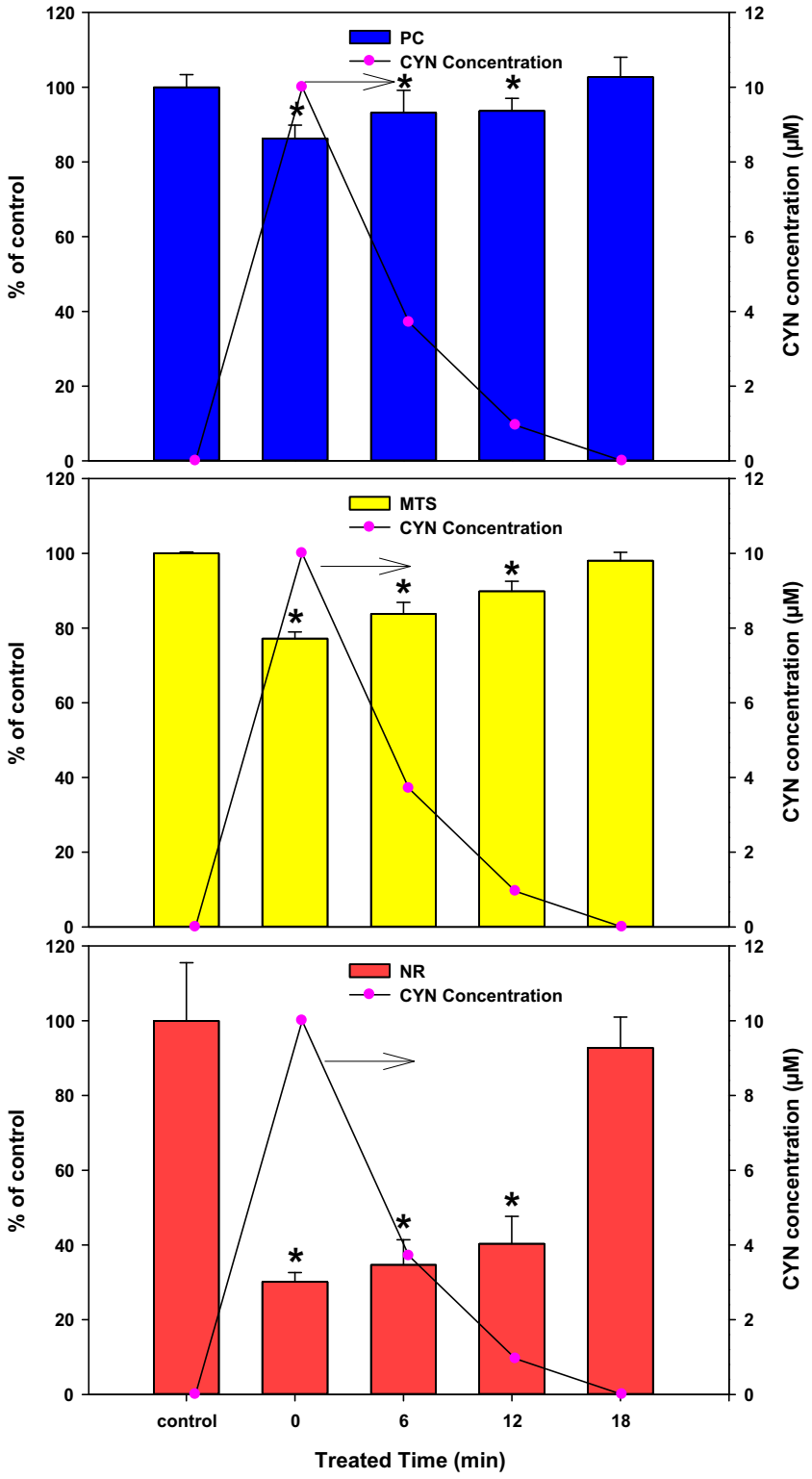

Fig. 1. The Protein content (PC), tetrazolium salt reduction (MTS), and neutral red uptake (NR) of CYN sample with different treated time ("*" indicates significantly different from control ($p \leq 0.05$)). (For interpretation of the references to color in this figure legend, the reader is referred to the web version of this article.)

3.2.3. Reaction on the hydroxymethyl uracil moiety

The detection of byproduct *m*/*z* 392.12 (Scheme 3) indicates the ring opening reaction on the uracil moiety related to the C5–C6 double bond. This byproduct can likely be derived from the hydroxyl addition byproduct of the C5–C6 double bond, such as *m*/*z* 432.12b which can have further oxidation to yield a diacid (*m*/*z* 466.12, not detected). Munk et al. proposed 5-OH-OG (hydroxylated 8-oxoguanine) can realize ring opening by loss of carbon dioxide derived from the carbonyl group most probably through the formation of an isocyanate and then a carbamic acid byproduct [43]. The proposed structure corresponding to *m*/*z* 466.12 can lose one mole of carbon dioxide (C4) from the carbamic acid group to form an amide group and a second mole of carbon dioxide from the carboxylic acid group (C5) to form a secondary alcohol group [20]

which can undergo oxidation to yield *m/z* 392.12 (Scheme S1, SI). Moreover, the *m/z* 392.12 byproduct can be further hydroxylated to form *m/z* 408.12 and 424.11. For the byproducts, such as *m/z* 392.12, the uracil ring was opened and the uracil structure no longer exists. Hence, they are unlikely to have toxicity originating from the uracil ring.

Another important byproduct related to the uracil ring opening is *m/z* 375.10. Its mass spectrum gives only two main fragments *m/z* 295.14 (−80 Da) and 277.13 (−18 Da), indicating the existence of the sulfate group and one hydroxyl group. Apparently, no more information is available from the mass spectrum. The retention time for this byproduct (1.28 min), which is longer than *m/z* 392.12, implies it has lower polarity. Therefore, a reformed ring structure is proposed (Fig. S8, SI). The cyclization with the presence of •OH was proposed in many research studies [44–46]. Here *m/z* 392.12 can be oxidized, transforming the amide group (N3–C2) to a carboxyl group [33,34], to form *m/z* 393.11 (not detected). By losing one molecule of H_2O, the *m/z* 375.10 byproduct can be generated (Scheme 3) [44]. Song et al. also found a byproduct (P_{374}, $C_{14}H_{22}N_4O_6S$, *m/z* 375.13) and proposed a structure [12]. However, the *m/z* 375.10 in this study is a different byproduct with thirteen carbons different from P_{374} due to the mass difference of the molecule. This byproduct was also found in other studies [13,47].

The MS spectrum of byproduct *m/z* 322.11 ($C_{11}H_{19}N_3O_6S$) only confirmed the presence of one sulfate group (−80 Da) and two hydroxyl groups (−18 Da × 2). The oxidation of C7 can form an aldehyde or a corresponding geminal diol. The unsaturation number of this byproduct *m/z* 322.11 is 4, which can be attributed to the three rings and one double bond in the tricyclic guanidine moiety. Besides, the double bond of guanidine structure is very stable and addition reactions are unlikely [27]; the ring opening process on the tricyclic guanidine moiety would retain the unsaturation since a aldehyde or ketone would be generated (similar as the situation discussed later in 3.2.4). If byproduct *m/z* 322.11 has an aldehyde group at C7, the unsaturation would increase to 5, therefore, a geminal diol structure is proposed here, which is consistent with our previous research [13]. Since the geminal diol *m/z* 322.11 was found in all samples, it should be more stable than its aldehyde form (*m/z* 304.10), which only appeared in a few samples with very low peak area. Byproduct *m/z* 322.11 can be obtained from *m/z* 392.12 oxidation or from *m/z* 375.10 by losing one ammonia (N1) and two carbon dioxide molecules (C2 and C6) (Scheme 3) [33]. The *m/z* 322.11 can be further hydroxylated and/or sulfate eliminated to form *m/z* 338.10, 354.10, 370.09, 240.13, 256.13, 272.12 and 288.12. The byproduct *m/z* 320.09 is proposed to be the corresponding dehydrated byproduct of *m/z* 322.11. Under current observation, the *m/z* 320.09 should not have a carboxyl acid group due to the absence of fragment (−45 Da) derived from carboxyl acid group in its mass spectrum [22]. This byproduct also can have hydroxylation byproducts, such as *m/z* 336.09 and 352.08.

3.2.4. Reaction on the tricyclic guanidine moiety

By losing C7 from the byproducts discussed before, such as *m/z* 322.11, the byproducts *m/z* 292.10a and *m/z* 290.08 can be generated. The *m/z* 292.10a should be the corresponding alcohol of the ketone *m/z* 290.08 (Scheme 4). However, the *m/z* 292.10a can transform to be *m/z* 292.10b [48,49], which is a ring opening process (but the unsaturation remains the same by forming a carbonyl group on C8). The retention time of *m/z* 292.10a was slightly longer than *m/z* 290.08 and *m/z* 292.10b most likely because the hydroxyl group on C8 could even the distribution of electron density in molecule and decrease the polarity of the whole structure. They can also have hydroxylation byproducts, such as *m/z* 308.09 and 324.09 (for *m/z* 292.10), and *m/z* 306.08, 322.07 and 338.06 (for *m/z* 290.08), as well as dehydration byproducts, such as *m/z* 288.06. Similarly, they can have sulfate group elimination byproducts, i.e. *m/z* 208.11 and 210.12, and the corresponding hydroxylation byproducts, such as *m/z* 224.10, 226.12, 240.10, 242.11, 256.09 and 258.11. The *m/z* 292.10b can have further oxidation to lose C8 [20] and generate *m/z* 294.08 with carboxyl acid group. The *m/z* 294.08 can be hydroxylated to be *m/z* 310.07 and then be dehydrolyzed to form *m/z* 292.06 [44] (Scheme 4).

3.3. Detoxification by TiO_2 photocatalysis

C3A cells were chosen for detoxification studies due to their superior sensitivity to CYN [50]. Upon exposing C3A cells to concentrations of untreated CYN ranging from 0 to 10 μM, all measurements of cell viability (protein content (PC), tetrazolium salt reduction (MTS), and neutral red cellular uptake (NR)), decreased with increasing CYN concentration (Fig. S9 (SI)). Among these three assays, the NR assay showed the most response to the presence of untreated CYN with an 80% decrease in cell viability, a result seen in other CYN cytotoxicity studies [51]. C3A cells exposed to untreated CYN demonstrated diminished MTS reduction capability with 10 μM CYN resulting in a 35% decrease, consistent with other results showing CYN exposure resulted in lower metabolic activity [50] and reduced cell viability. Compared to the other two assays, the PC assay was less sensitive to CYN exposure, with PC only decreasing by about 19%.

In the detoxification study, C3A cells were exposed to the treated CYN with different photocatalytic time scales (Fig. 1). The HPLC result shows the 10 μM CYN can be completely removed after a treatment time of 18 min. All measures of cell viability increased with treatment time (0–18 min), indicating that the TiO_2 photocatalytic treatment resulted in reduced cytotoxicity. The CYN and associated byproducts generated after 18 min of photocatalytic treatment showed no significant difference from control cells unexposed to the toxin ($p > 0.05$), suggesting the TiO_2 photocatalysis process effectively removed and detoxified CYN. However, due to the acute toxicity of CYN, extended treatment time may be added to ensure no residual remains.

4. Conclusions

The reaction byproducts generated during the TiO_2 photocatalytic degradation of CYN with titania catalysts P25 and lab synthesized PM-TiO_2 were elucidated using LC/Q-TOF–ESI–MS. This study theorized and presented the reaction pathways and mechanisms of CYN degradation based on hydroxyl radical attack, including hydroxylation, sulfate elimination and ring opening reactions on the hydroxymethyl uracil moiety and tricyclic guanidine moiety. The reactions on the hydroxymethyl uracil moiety, such as hydroxylation and ring opening, are likely to reduce or eliminate the toxicity since hydroxymethyl uracil is mainly responsible for the toxicity of CYN. The detoxification study showed that CYN can be effectively remediated after only a short TiO_2 photocatalytic treatment. This study provides a fundamental support for the assessment and efficacy of CYN degradation using TiO_2 photocatalysts and enriches the understanding of CYN toxicity, laying the foundation for further regulations.

Acknowledgements

This US-Egypt collaborative study is funded by the U.S. Department of Agriculture (58-3148-1-152). G. Zhang is also thankful to China Scholarship Council (CSC) Scholarships (2009617129) for providing financial support towards her Ph.D. studies.

Appendix A. Supplementary data

Supplementary data associated with this article can be found, in the online version, at http://dx.doi.org/10.1016/j.apcatb.2014.08.034.

References

[1] P.R. Hawkins, M.T.C. Runnegar, A.R.B. Jackson, I.R. Falconer, Appl. Environ. Microbiol. 50 (1985) 1292–1295.
[2] K. Terao, S. Ohmori, K. Igarashi, I. Ohtani, M.F. Watanabe, K.I. Harada, E. Ito, M. Watanabe, Toxicon 32 (1994) 833–843.
[3] E. Bazin, S. Huet, G. Jarry, L. Le Hegarat, J.S. Munday, A.R. Humpage, V. Fessard, Environ. Toxicol. 27 (2012) 277–284.
[4] H. Lopez-Alonso, J.A. Rubiolo, F. Vega, M.R. Vieytes, L.M. Botana, Chem. Res. Toxicol. 26 (2013) 203–212.
[5] A.R. Humpage, F. Fontaine, S. Froscio, P. Burcham, I.R. Falconer, J. Toxicol. Environ. Health, A: Curr. Issues 68 (2005) 739–753.
[6] A.R. Humpage, I.R. Falconer, Environ. Toxicol. 18 (2003) 94–103.
[7] P. Senogles, G. Shaw, M. Smith, R. Norris, R. Chiswell, J. Mueller, R. Sadler, G. Eaglesham, Toxicon 38 (2000) 1203–1213.
[8] P.J. Senogles, J.A. Scott, G. Shaw, H. Stratton, Water Res. 35 (2001) 1245–1255.
[9] T. Fotiou, T. Triantis, T. Kaloudis, A. Hiskia, Chemosphere (2014), http://dx.doi.org/10.1016/j.chemosphere.2014.04.045, in press.
[10] R. Banker, S. Carmeli, M. Werman, B. Teltsch, R. Porat, A. Sukenik, J. Toxicol. Environ. Health, A: Curr. Issues 62 (2001) 281–288.
[11] R.L. Norris, G.K. Eaglesham, G. Pierens, G.R. Shaw, M.J. Smith, R.K. Chiswell, A.A. Seawright, M.R. Moore, Environ. Toxicol. 14 (1999) 163–165.
[12] W.H. Song, S.W. Yan, W.J. Cooper, D.D. Dionysiou, K.E. O'Shea, Environ. Sci. Technol. 46 (2012) 12608–12615.
[13] X. He, G. Zhang, A.A. de la Cruz, K.E. O'Shea, D.D. Dionysiou, Environ. Sci. Technol. 48 (2014) 4495–4504.
[14] G. Zhang, M.N. Nadagouda, K. O'Shea, S.M. El-Sheikh, A.A. Ismail, V. Likodimos, P. Falaras, D.D. Dionysiou, Catal. Today 224 (2014) 49–55.
[15] C. Han, M. Pelaez, V. Likodimos, A.G. Kontos, P. Falaras, K. O'Shea, D.D. Dionysiou, Appl. Catal., B: Environ. 107 (2011) 77–87.
[16] M.M. Bradford, Anal. Biochem. 72 (1976) 248–254.
[17] E. Borenfreund, J. Puerner, J. Tissue Cult. Methods 9 (1985) 7–9.
[18] R. Guzman-Guillen, A.I.P. Ortega, I. Moreno, G. Gonzalez, M.E. Soria-Diaz, V. Vasconcelos, A.M. Camean, Talanta 100 (2012) 356–363.
[19] D.C. Hurum, A.G. Agrios, K.A. Gray, T. Rajh, M.C. Thurnauer, J. Phys. Chem. B 107 (2003) 4545–4549.
[20] M.G. Antoniou, J.A. Shoemaker, A.A. De La Cruz, D.D. Dionysiou, Environ. Sci. Technol. 42 (2008) 8877–8883.
[21] M.G. Antoniou, J.A. Shoemaker, A.A. de la Cruz, D.D. Dionysiou, Toxicon 51 (2008) 1103–1118.
[22] R.M.W. Silverstein, X. Francis, David J. Kiemle, Spectrometric Identification of Organic Compounds, seventh ed., John Wiley & Sons, Hoboken, New Jersey, US, 2005.
[23] Q.O. Sun, Y.M. Xu, J. Phys. Chem. C 114 (2010) 18911–18918.
[24] T.H. Xie, J. Lin, J. Phys. Chem. C 111 (2007) 9968–9974.
[25] P. Salvador, J. Phys. Chem. C 111 (2007) 17038–17043.
[26] T. Tachikawa, M. Fujitsuka, T. Majima, J. Phys. Chem. C 111 (2007) 5259–5275.
[27] M.G. Antoniou, U. Nambiar, D.D. Dionysiou, Water Res. 43 (2009) 3956–3963.
[28] S. Kim, W. Choi, Environ. Sci. Technol. 36 (2002) 2019–2025.
[29] B. Halliwell, J.M.C. Gutteridge, O.I. Aruoma, Anal. Biochem. 165 (1987) 215–219.
[30] G.V. Buxton, C.L. Greenstock, W.P. Helman, A.B. Ross, J. Phys. Chem. Ref. Data 17 (1988) 513–886.
[31] C.C. Chen, P.X. Lei, H.W. Ji, W.H. Ma, J.C. Zhao, H. Hidaka, N. Serpone, Environ. Sci. Technol. 38 (2004) 329–337.
[32] V. Augugliaro, M. Bellardita, V. Loddo, G. Palmisano, L. Palmisano, S. Yurdakal, J. Photochem. Photobiol., C: Photochem. Rev. 13 (2012) 224–245.
[33] W.M. Garrison, Chem. Rev. 87 (1987) 381–398.
[34] P. Calza, E. Pelizzetti, C. Minero, J. Appl. Electrochem. 35 (2005) 665–673.
[35] M. Carrier, C. Guillard, M. Besson, C. Bordes, H. Chermette, J. Phys. Chem. A 113 (2009) 6365–6374.
[36] M. Carrier, N. Perol, J.M. Herrmann, C. Bordes, S. Horikoshi, J.O. Paisse, R. Baudot, C. Guillard, Appl. Catal., B: Environ. 65 (2006) 11–20.
[37] P.L. Carl, P.K. Chakravarty, J.A. Katzenellenbogen, J. Med. Chem. 24 (1981) 479–480.
[38] S.A. Chen, C.C. Tsai, Macromolecules 26 (1993) 2234–2239.
[39] B.N. Nukuna, M.B. Goshe, V.E. Anderson, J. Am. Chem. Soc. 123 (2001) 1208–1214.
[40] S. Fujita, S. Ststeenken, J. Am. Chem. Soc. 103 (1981) 2540–2545.
[41] J. Bachman, H.H. Patterson, Environ. Sci. Technol. 33 (1999) 874–881.
[42] A. Samuni, P. Neta, J. Phys. Chem. 77 (1973) 2425–2429.
[43] B.H. Munk, C.J. Burrows, H.B. Schlegel, J. Am. Chem. Soc. 130 (2008) 5245–5256.
[44] J.R. Wagner, C. Decarroz, M. Berger, J. Cadet, J. Am. Chem. Soc. 121 (1999) 4101–4110.
[45] B. Ohtani, B. Pal, S. Ikeda, Catal. Surv. Asia 7 (2003) 165–176.
[46] K.V.S. Rao, B. Srinivas, A.R. Prasad, M. Subrahmanyam, Chem. Commun. (16) (2000) 1533–1534.
[47] S. Merel, M. Clement, A. Mourot, V. Fessard, O. Thomas, Sci. Total Environ. 408 (2010) 3433–3442.
[48] W.M. Garrison, M.J. Kland-English, H.A. Sokol, M.E. Jayko, J. Phys. Chem. 74 (1970) 4506–4509.
[49] C. Sheu, C.S. Foote, J. Am. Chem. Soc. 117 (1995) 4726.
[50] S.M. Froscio, S. Fanok, A.R. Humpage, J. Toxicol. Environ. Health, A: Curr. Issues 72 (2009) 345–349.
[51] D. Gutierrez-Praena, S. Pichardo, A. Jos, A.M. Camean, Ecotoxicol. Environ. Saf. 74 (2011) 1567–1572.